Extension of high-beta plasma operation to low-collisionality regime

Extension of High-beta Plasma Operation to low collisional Regime

S. Sakakibara[1,2], K.Y. Watanabe[1], H. Funaba[1], Y. Suzuki[1,2], S. Ohdachi[1,2], K. Ida[1,2], K. Tanaka[1], T. Tokuzawa[1], T. Morisaki[1,2], M. Osakabe[1,2], Y. Takeiri[1,2] and LHD Experiment Group

[1]National Institute for Fusion Science (NIFS), National Institutes for Natural Sciences (NINS), Toki 509-5292, Japan

[2]SOKENDAI (The graduate university for advanced studies), Toki 509-5292, Japan

E-mail: sakakibara.satoru@lhd.nifs.ac.jp

Abstract. In Large Helical Device (LHD), plasma with more than 4% average beta was successfully produced by multi-pellet injections in one order of magnitude lower collisional regime than that of previous high-beta operations. An improvement of particle confinement was observed during a high-beta discharge produced by gas-puff, and then particle flux to divertor was reduced by more than 40%. Strong instabilities at plasma edge appeared then and suppressed an increment of averaged beta to 3.4%. Spontaneous change of the magnetic topology contributes to the increase in averaged beta value, while it triggers excitation of edge MHD instabilities.

1. Introduction

Production of high beta plasma is one of the common issues in magnetic confinement systems for realization of economical fusion reactor. In currentless plasmas of stellarator/heliotrons, suppression of pressure-driven instabilities and preservation of robust magnetic field structures are key subjects for increasing the beta value. The weak magnetic shear and/or strong magnetic hill configurations easily destabilize interchange mode, which lead to significant reduction of the beta value [1]. Also, it is predicted that the increase in beta value leads to stochastization of magnetic field structure in periphery, which reduces available plasma confinement region [2]. The characteristics of MHD stability and equilibrium in high-beta plasmas are compared in Large Helical Device (LHD) and W7-AS stellarator through the International Stellarator/Heliotron Confinement Database activity [3, 4].

Since 1998, we have made high-beta experiments in Large Helical Device (LHD) to verify the potential of the high beta plasma production in stellarator/heliotrons. Achieved beta value had increased year by year, by an increment of heating power and the optimization of magnetic configurations for MHD stability, equilibrium and heating efficiency, and the beta value of more than 5% was successfully achieved [5]. Also the beta dependences of MHD stability and equilibrium had been experimentally studied in the wide beta range [6].

Previous experiments had been done in the high collisional regime because of low magnetic field operation at 0.425 T. To investigate the collisionality dependence of plasma confinement property, we have made high beta experiments in relatively high-field configurations at 1 T to increase the electron temperature. It is expected that an increase in the electron temperature raises magnetic Reynolds number, S, which contributes to suppression of low-n resistive interchange mode [5]. Also recovery of plasma confinement is expected because plasma confinement in the high collisional regime (< 0.5 T) gradually decrease with the beta value, which is predicted to be due to resistive-g turbulence with the same S dependence as the case of the low-n interchange mode [7].

Here we report the recent results of high-beta experiments in LHD. The high-beta discharges were produced by multi-pellet injections or gas-puff fueling. The magnetic configurations, heating devices and diagnostics are introduced in section 2. As the experimental results, high-beta plasma production

and MHD characteristics are described at section 3. In section 4, the obtained knowledge is discussed and summarized.

2. Experimental Setup

The LHD is a heliotron device with a pair of helical coils and three pairs of poloidal coils. All of coils are superconductive [8]. The typical major and minor radii are 3.6 m and 0.65 m, respectively. The toroidal magnetic field at R_{ax}^v, B_t, is less than 3 T, where R_{ax}^v is a preset magnetic axis position in vacuum and can be set at 3.5-4.1 m. The plasma aspect ratio, A_p, can be changed from 5.8 to 8.3 by controlling central position of helical coil currents [9].

Previous high-beta experiments had been done in configuration with R_{ax}^v of 3.6 m, B_t of -0.425 T and A_p of 6.6. In the experiments, the configuration with R_{ax}^v of 3.56 m, B_t of -1 T and A_p of 5.8 was applied for production of high-beta plasma, which was decided by results of R_{ax}^v scan experiments with constant heating power and constant electron density. The target plasmas were produced and maintained by three tangential neutral beams (NBs) and two perpendicular NBs. The total port-through power was about 25 MW. The ICRF heating with 3 MW was applied to increase the beta value. The volume averaged beta value, $<\beta>$, is estimated by the diamagnetic flux measurement. Profiles of electron temperature and density are measured with Thomson scattering system, and line averaged electron density is obtained by the measurement of FIR interferometer. Ion saturation currents, density and temperature on divertor plate are measured with Langmuir probes array.

3. Experimental Results

Figure 1 shows achieved beta value in different collisionality. In the previous high beta experiments, $<\beta>$ of 5.1% was obtained in the plasmas with $\nu_h^* \sim 1000$ at 0.425 T, where ν_h^* is normalized collisionality. FY2014 experiments had been done at 1 T, and the optimum magnetic configuration for high-beta plasma production was explored. Consequently, $<\beta>$ of 4.1% was achieved in the plasma with $T_{e0} \sim 0.9$ keV and $\nu_h^* \sim 100$ produced by the multi-pellet injections, and $<\beta> \sim 3.4\%$ and $\nu_h^* \sim 20$ were realized by gas-puff. T_{e0} reached 1.2 keV then. Achieved parameters, configurations and characteristics of obtained plasmas are summarized at Table 1. In the discharge with multi-pellet injections, peaked pressure profile is formed which excites core instability, whereas broaden profile leads to destabilization of edge instabilities in the gas-puff discharge. An improvement of particle confinement was observed in the gas-puff discharge although it is unclear in the pellet case because of short duration time of the discharge. A long-time duration in the pellet discharge and the stability control in the gas-puff one are subjects to be solved in the future.

The results of experiments with the multi-pellet injections and the gas-puff are described at section 3.1 and 3.2, respectively. Comparison of MHD characteristics in between A_p of 5.8 and 6.6 (previous high-beta configuration) is shown at section 3.3.

TABLE I: SUMMARY OF HIGH-BETA EXPERIMENTS

	Pellet discharge	Gaspuff discharge
Achieved $<\beta>$	4.1%	3.4%
Duration Time	< 0.1s	>0.5s (limited by heating)
T_{e0}	0.9 keV (0.2 keV at 0.425 T)	1.2 keV (0.5 keV at 0.425 T)
n_{e0}	6×10^{19} m^{-3}	3×10^{19} m^{-3}

Pressure profile	Peaked profile	Broad profile
Improvement of particle confinement	unclear	observed
Instability	core mode	edge mode
Issues	long time duration	stability control fueling to core

3.1 High-beta discharge with multi-pellet injections

Figure 2 show the typical high-beta discharge with multi-pellet injections. Three tangential neutral beams (NBs) were injected from 3.3 s and the two perpendicular NBs were added at 3.7 s. The ICRF heating was applied at 3.7-4.2s. The pellets were injected four times during 3.62-3.72s. The $<\beta>$ reaches 4.1% at 3.78s and then central beta is about 7%. The electron density was increased with pellets and started to decrease at 3.75 s. The profiles of electron temperature and density are shown in Fig.3. Both the temperature and the density have peaked profiles, which cause large Shafranov shift. The R_{ax} is set at 3.56 m and is shifted to 4.0 m.

The temporal changes of the amplitude of $m/n = 2/1$ mode and the peaking factor of the beta profile are shown in Fig.4, where m and n are poloidal and toroidal mode number, respectively. The $m/n = 2/1$ mode appeared and grew at 3.75 s, and the amplitude starts to decrease with reduction of the peaking factor. The equilibrium calculation by HINT2 code show that the resonant surface of $m/n = 2/1$ mode is located at $\rho \sim 0.5$ ($R \sim 3.5$ and 4.3m). It is predicted that the increment of the peaking factor corresponds to the increase in the pressure gradient around the resonance. In the discharge, amplitudes of MHD modes excited in the plasma edge are very small compared to the gas-puff case (see section 3.2).

3.2 High beta discharge with gas-puff

Figure 5 shows the typical gas-puff discharge. The discharge condition is almost the same as the Fig.2 discharge except for the fueling method. After the electron density, $<\beta>$, Hα increase at 3.7s with additional heating, the density and beta start to increase further at 3.76s. Here we define this phenomenon "transition" [10]. Then fluctuation of Hα signal appears and $m/n = 1/2$ mode located at plasma edge is excited. The mode seems to suppress the increment of the $<\beta>$.

Profiles of electron density and temperature at 3.733, 3.8 and 3.866 s of Fig.5 discharge are shown in Fig.6. The R_{ax} is about 3.8 m. After the transition, the electron density at $R = 4.3$-4.8 m increases, which forms significant hollow profile. The electron temperature profile is not changed before and after the transition. Figure 7 shows the electron pressure profiles at 3.733, 3.8 and 3.866 s. The plasma confinement region seems to be expanded to the outward.

Figure 8 shows the time evolutions of beta value, ion saturation current, electron density and temperature on the divertor plate. The transition occurs at 3.8 s, and then ion saturation current, density and temperature significantly drop, which suggest that the improvement of the particle confinement is realized.

The discharge before and after the transition is extended in Fig.9. At 3.79 s, Hα signal and ion saturation current start to decrease, and $<\beta>$ starts to increase at 3.8s. When $<\beta>$ reaches the maximum at 3.82s, the fluctuation of Hα signal appears. The fluctuations of both Hα and ion saturation current are caused by the fluctuation of MHD mode. Although the reduction of Hα signal suggests the transition to confinement improved mode, the excitation of MHD instability suppress the increase in $<\beta>$.

The $m/n = 2/3$ and/or 1/2 modes excited in the plasma edge were enhanced after the transition, which limit the achieved beta value. Figure 10 shows profiles of plasma pressure, rotational transform and connection length of magnetic field line before and after the transition, which was calculated by using HINT2 code. After the transition, pressure profile was radially spread and the connection length was increased at $R > 4.57$ m. It suggests that enhancement of edge MHD instabilities are due to spontaneous

appearance of rational surface with sufficiently long connection length, which means that magnetic field structure is changed from stochastic to nested one and it leads to the extension of plasma confinement region. One possibility is that the stochastic magnetic field formed by high-n magnetic islands is healed by effects of beta, collisionality and so on [2]. This is discussed on section 4.

3.3 MHD characteristics in A_p=5.8 and 6.6 configurations.

Here we compare the discharge in the $A_p = 5.8$ configuration with that in the $A_p = 6.6$ case. The $R_{ax}{}^v$ is 3.56 m and $B_t = -1$ T in both cases, and the heating condition is the same. The $<\beta>$ is almost the same in both cases before the transition (3.76 s) as shown in Fig.11. The increase in $<\beta>$ after the transition is found in the $A_p = 5.8$ case, whereas no transition occurs in the $A_p = 6.6$ case. The R_{ax} shift in the $A_p = 5.8$ case is larger than that in the $A_p = 6.6$ case because the central rotational transform in the $A_p = 5.8$ case is higher than the case of $A_p = 6.6$ ($\iota/2\pi = 0.4$ at $A_p = 5.8$ and 0.55 at $A_p = 6.6$).

Figure 12 shows the difference of MHD activities in $A_p = 5.8$ and 6.6 discharges. As described in section 3.1, instabilities excited in the periphery ($m/n = 1/1$) and the edge ($m/n = 2/3$, $1/2$) are dominantly observed, especially after the transition, in the $A_p = 5.8$ case. In the $A_p = 6.6$ case, strong $m/n = 2/1$ mode excited in the core appeared and is enhanced with the increase in $<\beta>$. The edge instability with $m/n = 2/3$ appears, while the amplitude is relatively small because of no transition.

4. Discussion and Summary

The high-beta operation is extended towards low-collisional regime, which is important for extrapolation of obtained plasma characteristics to reactor-relevant regime. The volume averaged beta value of 4.1% was successfully obtained by the multi-pellet injections. The long-time sustainment of high-beta plasma is one of the subjects to be solved, which could be demonstrated by using repetitive pellet injections. The core instability due to formation of the peaked pressure profile is excited at the maximum beta. It is expected that the mode is suppressed by the magnetic well formation due to the increment of Shafranov shift with the beta value.

The quasi-steady state high beta discharge with more than 3 % was demonstrated in the relatively low-collisional regime, and improvement of particle confinement was obviously observed then. The analyses of equilibria before and after the transition suggest that the plasma confinement region is extended to the outward, which means that the stochastic magnetic field structure is changed to the nested one. Previous studies on the magnetic topology suggest that the formation of the magnetic island strongly depends on beta and collisionality [11-13]. If the stochastic magnetic field structure is formed by chain magnetic islands, disappearance of the magnetic island is one of the candidates to explain the change of magnetic topology. Since an appearance of "new" rational surface leads to excitation of MHD mode limiting the increase in the beta value, the stability control is one of the key issues on realization of higher beta plasma production. Also, this transition has no contribution to the increase in core pressure. The fueling technique using gas-puff and pellet injection should be considered in order to increase higher central beta value.

In summary, high-beta plasma with more than 4% was successfully produced by multi-pellet injections in one order lower collisional regime than that of previous high-beta operations in LHD. An improvement of particle confinement was observed during a high-beta discharge produced by gas-puff, and then particle flux to divertor was reduced by more than 40%. Strong instabilities at plasma edge appeared then and suppressed an increment of averaged beta to 3.4%. Spontaneous change of the magnetic topology contributes to the increase in averaged beta value, while it triggers excitation of edge MHD instabilities.

Acknowledgments

References

[1] SAKAKIBARA, S. et al., "Characteristics of MHD instabilities limiting the beta value in LHD", *Nucl. Fusion* **55** (2015) 083020.

[2] SUZUKI, Y. et al., "Effects of the Stochasticity on Transport Properties in High-β LHD", *Plasma Fusion Res*. **4** (2009) 036.

[3]   WELLER, A. et al., "International Stellarator/Heliotron Database progress on high-beta confinement and operational boundaries", *Nucl. Fusion* **49** (2009) 065016.

[4] STROTH, U., et al., "Energy confinement scaling from the International Stellarator Database" *Nucl. Fusion* **36** (1996)1063–77.

[5] SAKAKIBARA, S. et al., "MHD study of the reactor-relevant high-beta regime in the Large Helical Device", *Plasma Phys. Control. Fusion* **50** (2008) 124014.

[6] WATANABE K.Y. et al., "Effects of global MHD instability on operational high-beta regime in LHD", *Nucl. Fusion* **45** (2005) 1247-1254.

[5] FUNABA H., et al., "Local transport property of high-beta plasmas on LHD", Fusion Sci. Technol. **58** (2010) 141-149.

[6] KANEKO, O. et al., "Extension of operation regimes and investigation of three-dimensional currentless plasmas in the Large Helical Device", *Nucl. Fusion* **53** (2013) 104015.

[7] SAKAKIBARA, S. et al., "Study of MHD Stability in LHD", *Fusion Sci. Technol.* **58** (2010) 176-185.

[8] TOI, K. et al., "L-H transition and edge transport barrier formation on LHD", *Fusion Sci. Technol.* **58** (2010) 61-69.

[9]   NARUSHIMA Y. et al., "Dependence of spontaneous growth and suppression of the magnetic island on beta and collisionality in the LHD", *Nucl. Fusion* **48** (2008) 075010.

[10]   SAKAKIBARA, S. et al., "Modification of the magnetic field structure of high-beta plasmas with a perturbation field in the Large Helical Device", *Plasma Phys. Control. Fusion* **55** (2013) 014014.

[11]   SAKAKIBARA, S. et al., "Response of MHD stability to resonant magnetic perturbation in the Large Helical Device", *Nucl. Fusion* **53** (2013) 043010.

Figure Captions

Fig.1   Changes in achieved beta value as a function of collisionality

Fig.2   Typical high-beta discharge with multi-pellet injections.

Fig.3   Profiles of electron temperature and density at 3.8 s of Fig.2 discharge.

Fig.4   Temporal changes of amplitude of $m/n = 2/1$ mode and peaking factor.

Fig.5   Time evolutions of electron density, averaged beta, H$\square$ and amplitude of $m/n = 1/2$ mode in the gas-puff discharge (Shot#129303).

Fig.6   Profiles of electron density and temperature at 3.733, 3.8 and 3.866 s of Fig.5 discharge.

Fig.7   Electron pressure profiles at 3.733, 3.8 and 3.866 s of Fig.5 discharge.

Fig.8   Time evolutions of beta value, ion saturation current, electron density and electron temperature on the divertor plate (Shot#130541).

Fig.9   Extended view of temporal changes of beta, Ha and ion saturation current in Fig.6 discharge.

Fig.10   Profiles of electron pressure, rotational transform and connection length of magnetic field line before and after transition (Shot#129303, 3.73 s (before) and 3.76 s (after)).

Fig.11   Time evolutions of averaged beta and magnetic axis position in $A_p = 5.8$ and 6.6 discharges.

Fig.12   Time evolutions of averaged beta, frequencies and amplitude of observed MHD modes in $A_p = 5.8$ discharges.

Fig.13   Time evolutions of averaged beta, frequencies and amplitude of observed MHD modes in $A_p = 6.6$ discharges.
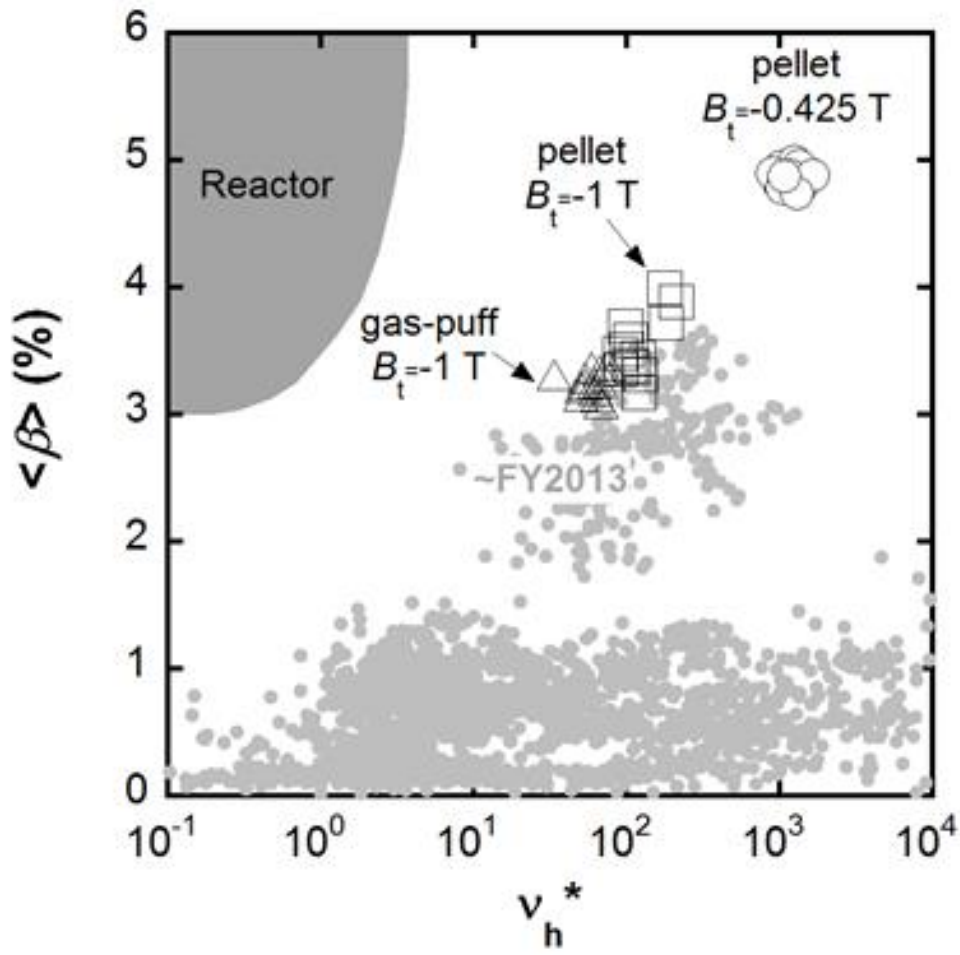
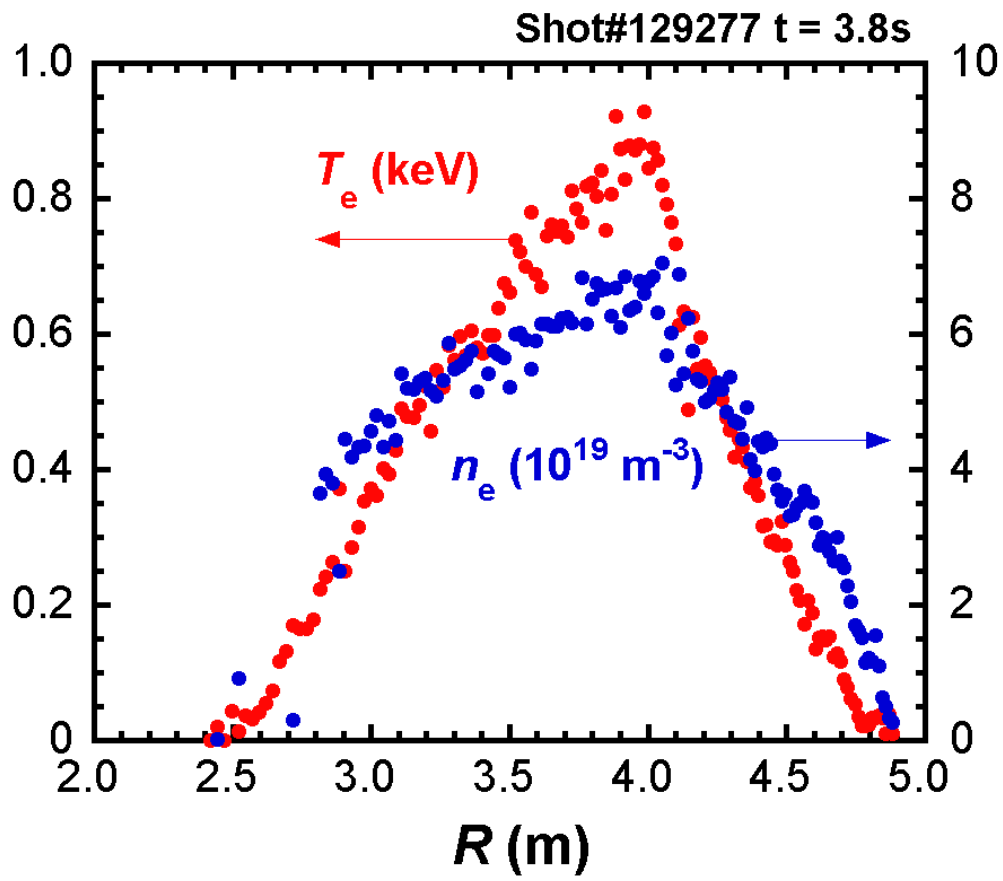Fig.1   S.Sakakibara et al.

Fig.2   S.Sakakibara et al.

Shot#129277 t = 3.8s

T_e (keV)

n_e (10^{19} m^{-3})

R (m)
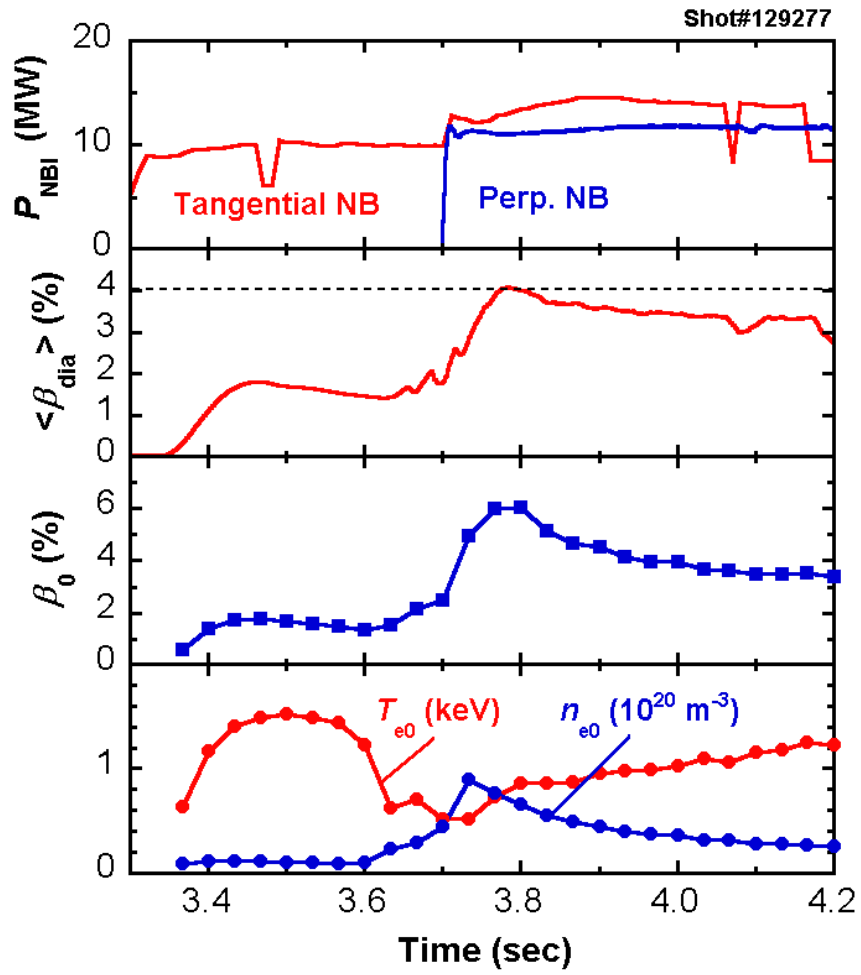
Fig.3   S.Sakakibara et al.

Fig.4   S.Sakakibara et al.

NBI+ICRF

$\overline{n}_e$ (10^{19} m^{-3})

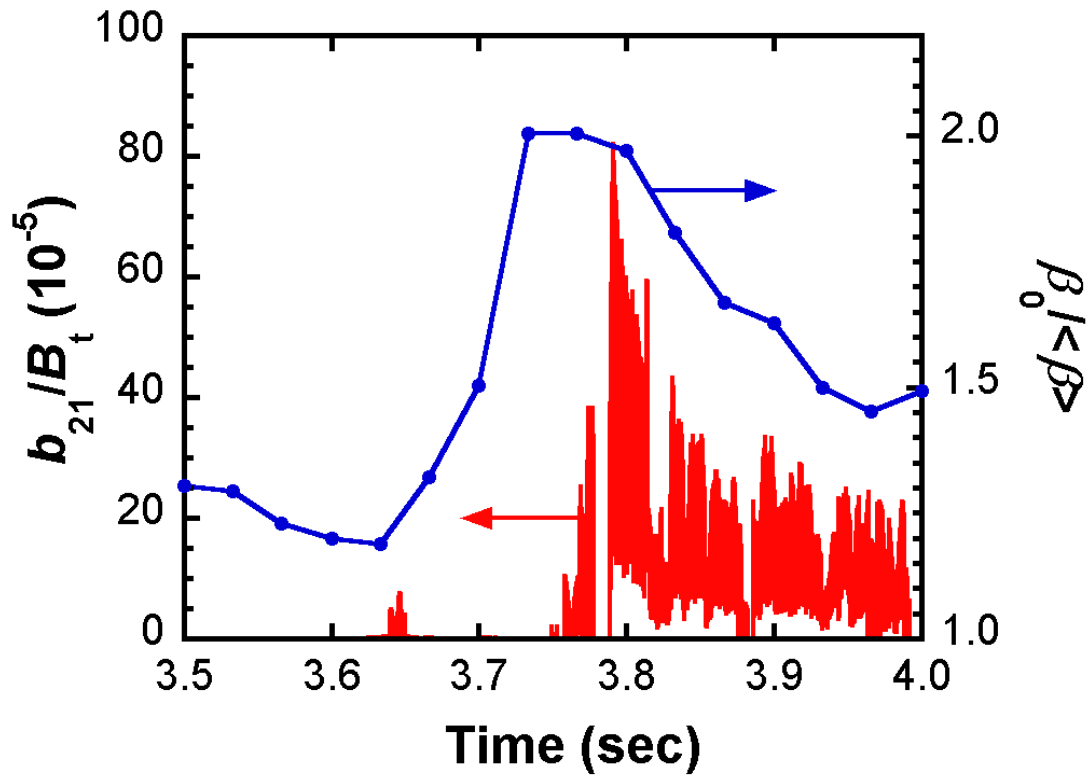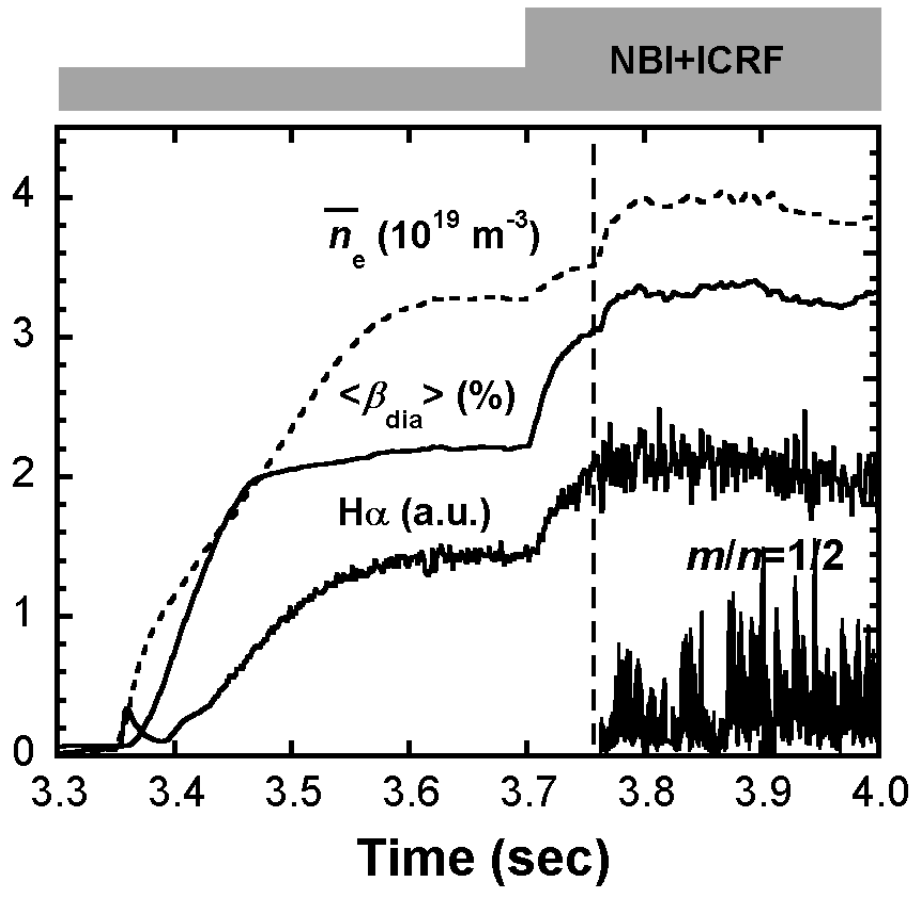$<\beta_{dia}>$ (%)

Hα (a.u.)
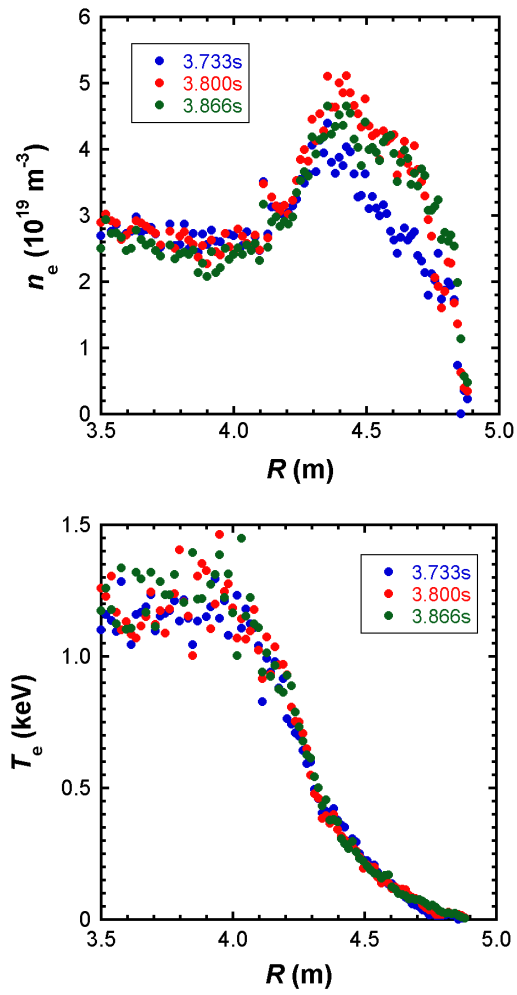
m/n=1/2

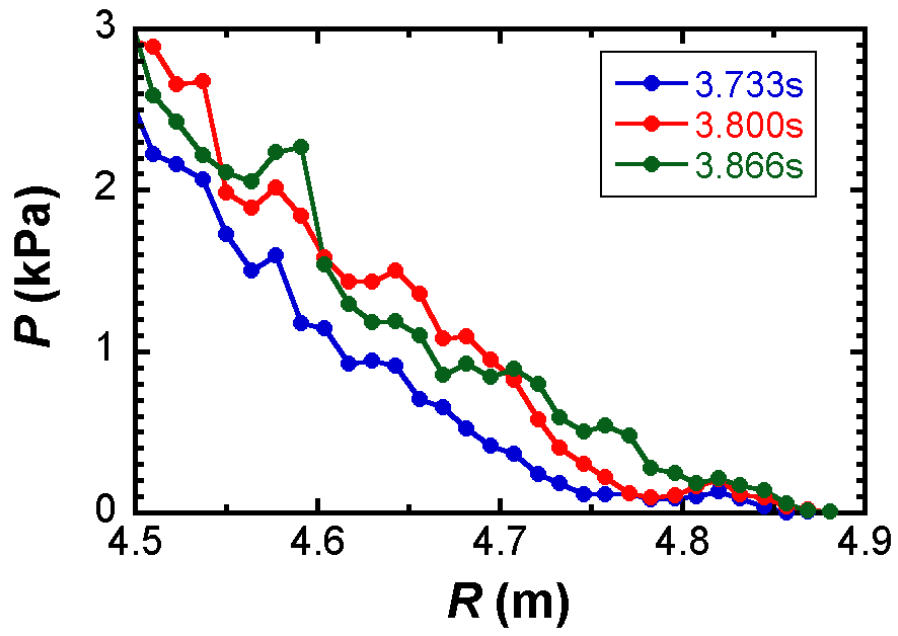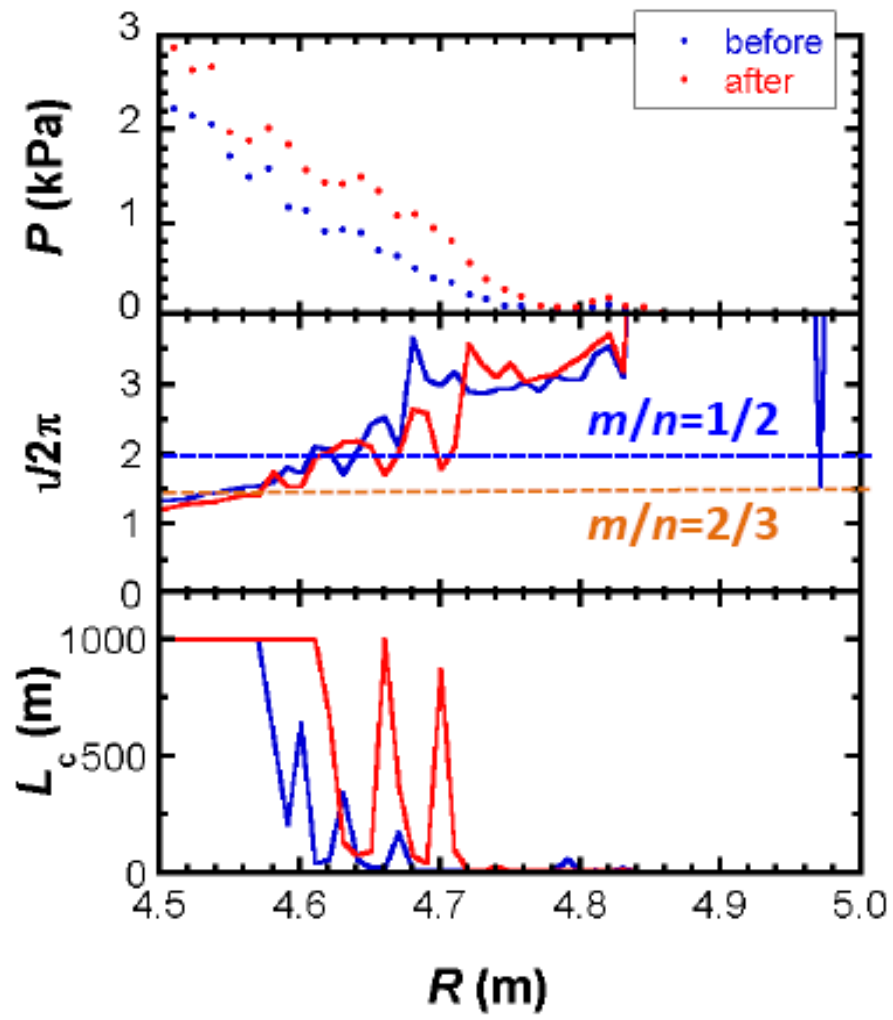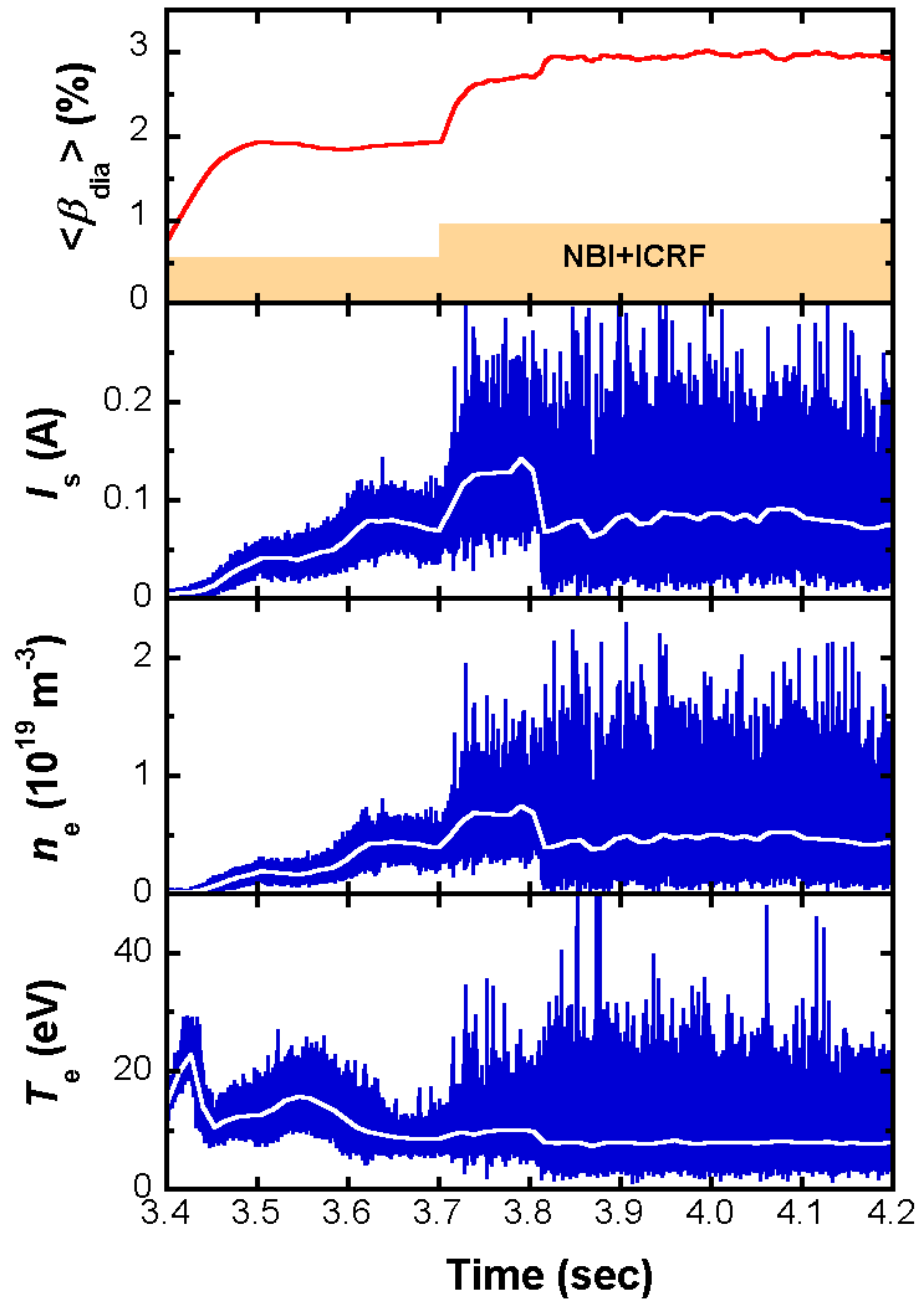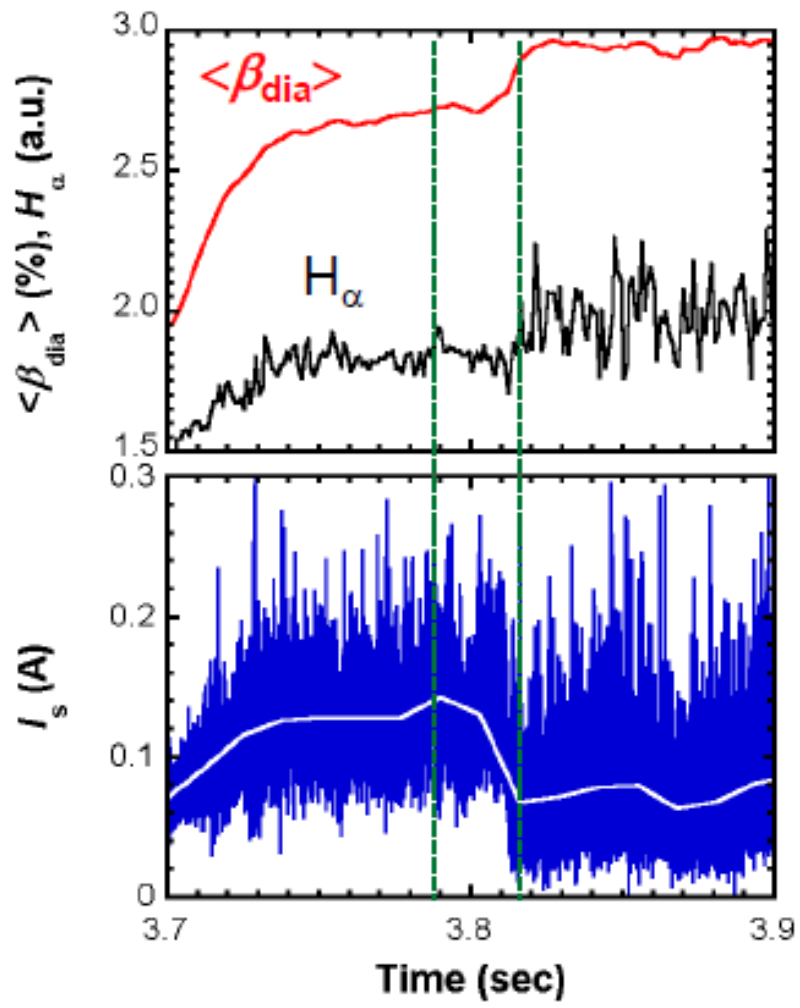Fig.5   S.Sakakibara et al.

Fig.6   S.Sakakibara et al.

Fig.7   S.Sakakibara et al.

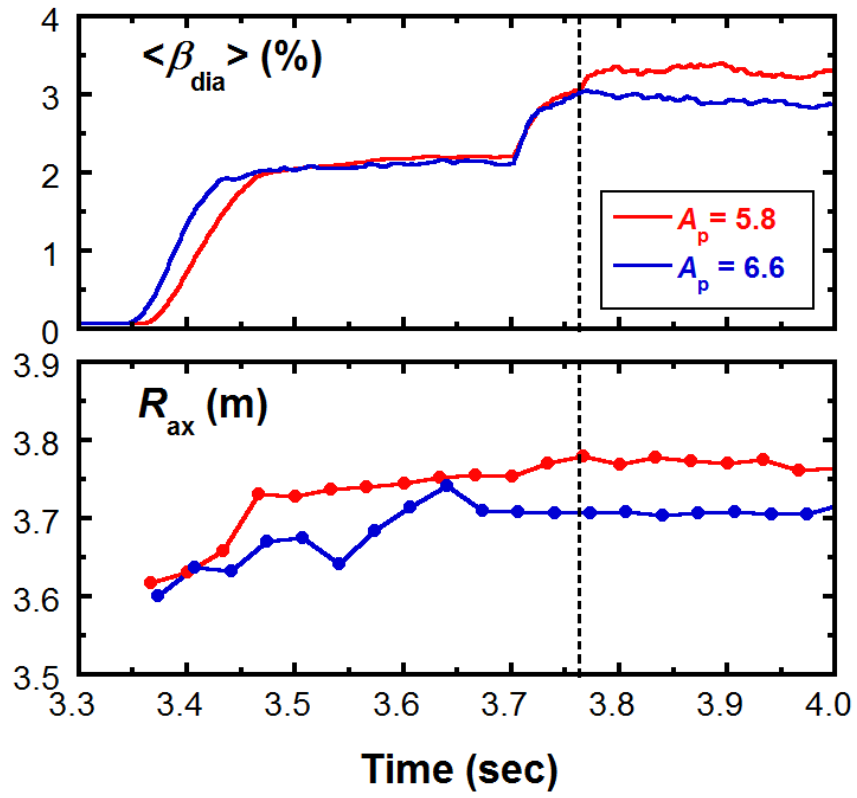Fig.8   S.Sakakibara et al.

Fig.9   S.Sakakibara et al.

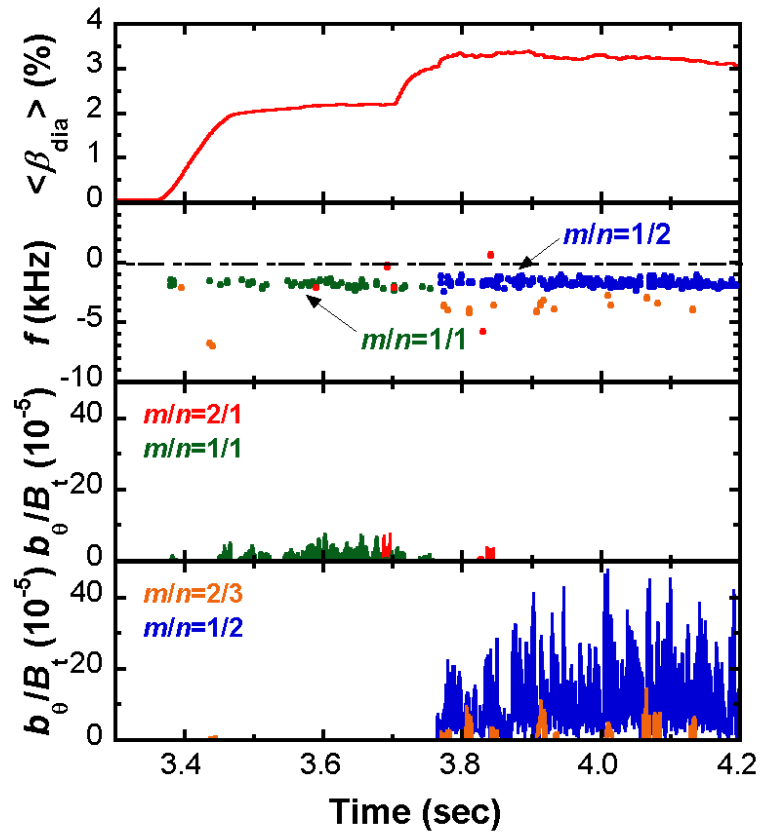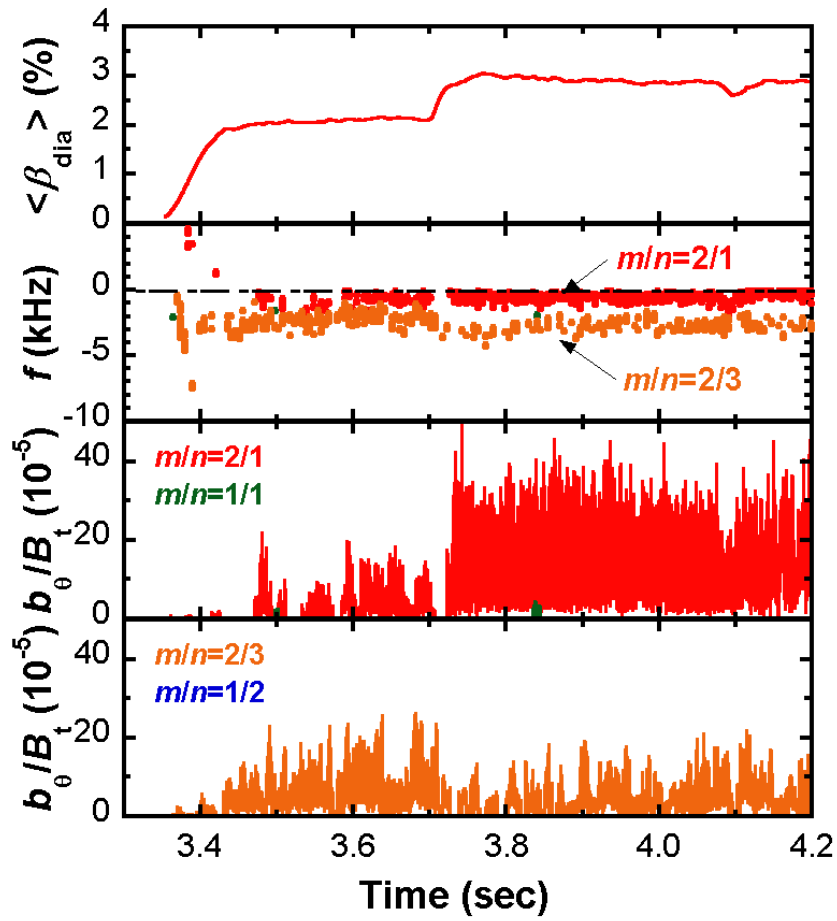Fig.10   S.Sakakibara et al.

Fig.11   S.Sakakibara et al.

Fig.12   S.Sakakibara et al.

Fig.13   S.Sakakibara et al.